doi:10.1016/j.jmb.2004.06.008 *J. Mol. Biol.* (2004) **341**, 27–36

JMB

Available online at www.sciencedirect.com

SCIENCE DIRECT®

ELSEVIER

Folding of the *Tetrahymena* Ribozyme by Polyamines: Importance of Counterion Valence and Size

Eda Koculi[1], Nam-Kyung Lee[2], D. Thirumalai[3]* and Sarah A. Woodson[1]*

[1]*T. C. Jenkins Department of Biophysics, Johns Hopkins University, 3400 N. Charles St. Baltimore, MD 21218, USA*

[2]*Institute of Fundamental Physics, Department of Physics Sejong University, Seoul 143-747 South Korea*

[3]*Institute for Physical Sciences and Technology, University of Maryland, College Park, MD 20742, USA*

**Corresponding authors*

Polyamines are abundant metabolites that directly influence gene expression. Although the role of polyamines in DNA condensation is well known, their role in RNA folding is less understood. Non-denaturing gel electrophoresis was used to monitor the equilibrium folding transitions of the *Tetrahymena* ribozyme in the presence of polyamines. All of the polyamines tested induce near-native structures that readily convert to the native conformation in Mg^{2+}. The stability of the folded structure increases with the charge of the polyamine and decreases with the size of the polyamine. When the counterion excluded volume becomes large, the transition to the native state does not go to completion even under favorable folding conditions. Brownian dynamics simulations of a model polyelectrolyte suggest that the kinetics of counterion-mediated collapse and the dimensions of the collapsed RNA chains depend on the structure of the counterion. The results are consistent with delocalized condensation of polyamines around the RNA. However, the effective charge of the counterions is lowered by their excluded volume. The stability of the folded RNA is enhanced when the spacing between amino groups matches the distance between adjacent phosphate groups. These results show how changes in intracellular polyamine concentrations could alter RNA folding pathways.

Keywords: RNA folding; counterion condensation; group I ribozyme; polyamines

Introduction

Interactions between counterions and RNA polyelectrolytes are critical for the self-assembly of RNA tertiary structures. Stabilization of RNA tertiary structure by metal ions such as Mg^{2+} has been studied extensively.[1] In the cell, polyamines such as spermine, spermidine and putrescine (Figure 1) also interact with nucleic acids.[2] Because polyamines are flexible cations with different charge and size, they have the potential to modulate RNA folding transitions in subtle ways. Moreover, because the chemical structures of polyamines are reminiscent of basic oligopeptides that interact with RNA,[3] the energetics of RNA folding in polyamines may provide insight into RNA–protein interactions.

Polyamines are ubiquitous, abundant, and essential for cell growth.[2] Because they stabilize condensed chromatin and interact with mRNAs and ribosomes, polyamines affect gene expression on many levels.[4,5] In fission yeast and mammals, polyamines inhibit their own synthesis by stimulating translational frameshifting that produces an inhibitor of ornithine decarboxylase, a key enzyme of polyamine biosynthesis.[6,7] Polyamine concentrations are elevated in some tumors, making polyamine biosynthesis a potential drug target.[8]

Like other multivalent cations, polyamines trigger DNA condensation,[9] and stabilize triple helices and DNA–RNA hybrids.[10–12] Polyamines also modulate the structure of tRNA and other RNAs,[5] although their role in RNA folding is still poorly understood. In crystallographic studies, polyamines have been found to interact with specific sites in double-stranded DNA[13] or tRNA.[14] Solutions studies, however, have shown that polyamines primarily interact non-specifically with the phosphate groups, diffusing freely within a prescribed volume around the DNA.[15–17] As is the case for metal cations, non-specific electrostatic interactions with "condensed" counterions

Abbreviations used: BD, Brownian dynamics.

E-mail addresses of the corresponding authors: swoodson@jhu.edu; thirum@glue.umd.edu

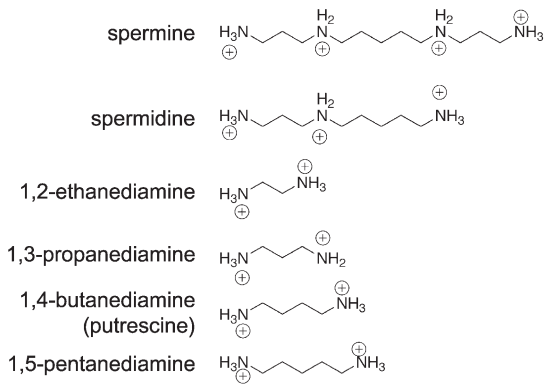

Figure 1. Chemical structures of polyamines used in this study.

dominate interactions between polyamines and nucleic acids.[9,18]

We previously used native gel electrophoresis to compare stabilization of the *Tetrahymena* L-21 ribozyme by various metal ions and spermidine.[19] Because only conformations close to the native state are trapped as the native form during electrophoresis,[20] this assay is sensitive to the tertiary structure of the RNA. Spermidine^{3+} stabilized the folded RNA less effectively than cobalt hexammine^{3+}, demonstrating that the size and geometry of the counterion is important in RNA folding.[19] In this study, we refolded the *Tetrahymena* ribozyme in a series of polyamines with differing charge and size (Figure 1). The results provide strong evidence that, besides dominant non-specific electrostatic interactions with the phosphate groups, the excluded volume and conformational entropy of counterions also make important contributions to the stabilization of RNA tertiary structure.

Relating counterion-induced collapse and folding

The earliest event in the folding of large RNA molecules is the transition from the unfolded state to an ensemble of compact structures.[21] This transition is preceded by the association of counterions and a reduction of more than 90% in the effective charge on the phosphate groups. The condensation of counterions around the RNA reduces the electrostatic repulsion between the phosphate groups, permitting attractive interactions to drive collapse of the RNA. After counterion condensation, there is a substantial reduction in the RNA's radius of gyration (R_g). This counterion-mediated collapse has been confirmed by recent small angle X-ray and small angle neutron scattering experiments on several RNAs.[22–26]

The Manning criterion for condensation of counterions,[27] which is accurate for infinite rod-like polyelectrolytes and spherical counterions, is $\frac{l_B}{b} > \frac{1}{Z}$, where $l_B = e^2/4\pi\epsilon k_B T \approx 7.1$ Å at $T = 25$ °C is the Bjerrum length, b is the typical distance between phosphate groups, and Z is the counterion valence. If the counterions are spherical then the effective average fractional charge, $\bar{\nu}$, that each phosphate carries upon counterion condensation can be estimated using the two-phase approximation. By equating the chemical potential of the free and condensed counterions, we obtained $N\bar{\nu} \cong -\ln \phi(R_g/l_B)(Z^{-1})$ for a globular RNA, where N is the number of nucleotides and ϕ is the volume fraction of counterions.[19] Multivalent counterions neutralize the phosphate charge on RNA more fully than monovalent ions,[19] consistent with results from DNA condensation.[28] As discussed below, multivalent ions also produce more compact structures by forming attractive interactions that bridge phosphate groups.[29,30]

It is now well accepted that the majority of neutralization of the phosphate charges comes from delocalized binding of cations.[28,31,32] In counterion condensation theory[27] or Poisson–Boltzmann theory,[33] the softened electrostatic interaction is described in terms of the reduced charge on the backbone ($-\bar{\nu}e$). Because the condensed counterions remain mobile, however, they fluctuate. Correlated charge fluctuations, which depend on Z and the shape of the counterions, produce an intermolecular attraction. The strength of the attractive potential is $\Delta \propto Z^2(\ell_B/b)^2 f_Z$, where f_Z is the fraction of condensed multivalent cation.[34] The condensation of counterions and charge fluctuations lead to a reduction in the persistence length of the RNA, which causes the RNA to adopt compact structures.

Role of counterion size and shape

The extent of compaction, which ultimately determines the thermodynamics and kinetics of RNA folding, is determined not only by valence but also by the size and shape of the counterions. This is because their interactions with other counterions and with the RNA vary, depending on the chemical structure of the counterion. These interactions are not static, but fluctuate due to conformational changes in the RNA and the mobility of counterions. For larger amines, greater correlations between the condensed counterions are expected, due to increased excluded volume. As a result, for the diamine series shown in Figure 1, we predict that the concentration required to obtain a similar $\bar{\nu}$ should increase as the size of the counterion increases, even though the counterion valence ($Z = 2$) remains constant.

Hence, the folding thermodynamics of RNA depends on the effective charge density ζ of the counterions:

$$\zeta = Z/A(T) \qquad (1)$$

where the second virial coefficient $A(T) = \int d\Omega_1 d\Omega_2 d^3R_{12}(1 - e^{-\beta U(\Omega_1,\Omega_2,R_{12})})$ and $\beta = (k_B T)^{-1}$. $U(\Omega_1, \Omega_2, R_{12})$ is the relative orientation and

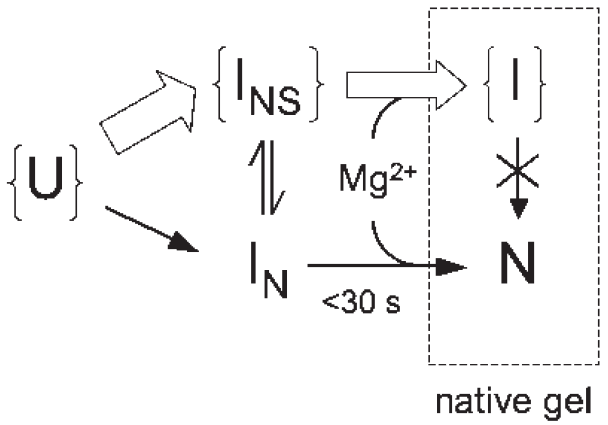

Figure 2. Native gel folding assay. When equilibrated with cations, the unfolded ribozyme (U) forms non-native (I_{NS}) and native-like (I_N) intermediates. I_N is converted to N in the presence of 3 mM $MgCl_2$ during a short exposure to 3 mM $MgCl_2$ in the running buffer.[19] The ensemble of I states are not converted to N during this time. Exchange between the native and non-native structures in the gel matrix is not observed during the electrophoresis at ≤10 °C.[20]

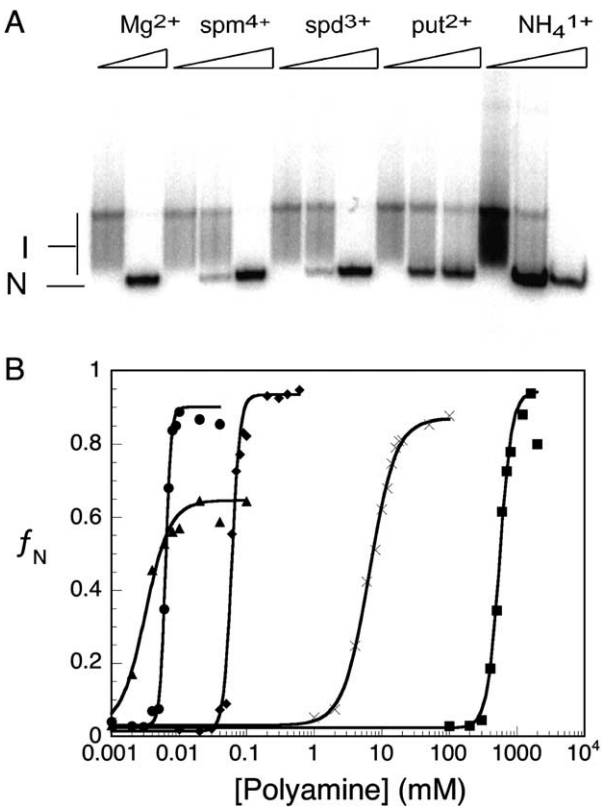

Figure 3. Equilibrium folding of the *Tetrahymena* ribozyme by amines of different charge. A, Uniformly α-^{32}P-labeled L-21 ribozyme was incubated in HE buffer plus various concentrations of polyamines or $MgCl_2$ at 30 °C for two to four hours before native 8% PAGE. I, misfolded RNA; N, native RNA. HE, buffer only; Mg^{2+}, 1.2 mM $MgCl_2$. Polyamine concentrations: 0 mM, 0.006 mM, 0.01 mM spermine·$(HCl)_4$ (spm); 0 mM, 0.06 mM, 0.3 mM spermidine·$(HCl)_3$ (spd); 0 mM, 6 mM, 100 mM putrescine·$(HCl)_2$ (put); 0 mM, 600 mM, 1600 mM NH_4Cl. B, Fraction of native RNA (f_N) *versus* polyamine concentration. Curves represent the best fit to equation (2). The ΔG, C_m, n_H from the fits are shown in Table 1. Symbols: (▲) pentalysine; (◆) spermidine; (●) spermine; (×) putrescine (1,4-butanediamine); (■) ammonium chloride.

distance-dependent potential between each pair of counterions. If the potential $U(\Omega_1, \Omega_2, R_{12})$ is short-range and only includes steric interactions, then $A(T) \approx V$ where V is the volume of the counterion. Despite the expected complexity of mechanisms by which polyamines and pentalysine mediate RNA collapse, we propose that the cooperativity of folding is determined by an interplay of the charge and excluded volume of the counterions.

Excluded volume effects on competitive binding of a multivalent counterion to charged surfaces and cylinders have been considered.[29,35] A key finding in these studies is that the shortest distance between the counterion and the macroion (i.e. the excluded volume of the counterion) plays a significant role in determining the binding equilibria. For flexible counterions such as polyamines, the loss of conformational entropy in the counterion also contributes to the binding energy. Consequently, large polyamines stabilize RNA double helices less than smaller cations,[36] extend the persistence length of DNA relative to metal cations,[37] and condense DNA less efficiently.[18,38,39] Light scattering experiments showed that the size of condensed DNA particles is sensitive to the geometry and size of polycation.[40] This can be explained by a lower density of positively charged groups around the nucleic acid, for counterions with a larger excluded volume.

Results

Native gel electrophoresis folding assay

We used native polyacrylamide gels to quantify the equilibrium folding transition of the *Tetrahymena* L-21 ribozyme as described.[41] Mg^{2+} is required to stabilize the catalytically active form of the ribozyme (N), which can be separated from misfolded intermediates (I) in a native gel (Figure 2). Other cations, however, produce near-native species (I_N) that are close in energy and structure to the native state.[19] These are readily converted to the native form during a short exposure (15–30 s) to Mg^{2+} in the gel running buffer. Because the free energy barriers between the misfolded intermediates and the native state are large, the ensemble of intermediates (I) does not convert to N in a short time at the 10 °C gel temperature, and are trapped as slowly migrating conformers. Once the RNA enters the polyacrylamide matrix, further refolding is largely arrested.[20,42]

In 25 mM Na–Hepes, 1 mM EDTA (HE) the ribozyme is largely unfolded, and the RNA appeared as a smear in non-denaturing polyacrylamide gels containing 3 mM $MgCl_2$ (lane 1, Figure 3A). When the ribozyme was allowed to fold in 1.2 mM $MgCl_2$ before native PAGE, it appeared as a narrow band of faster electrophoretic mobility (*N*). Incubation of the ribozyme in polyamines (spermine, spermidine or putrescine) or ammonium ion also produced a band with the same mobility as samples folded in Mg^{2+} (Figure 3A). Previous work showed that 70–80% of the ribozyme was active after similar treatment (four hours at 30 °C in spermidine, followed by addition of 3 mM $MgCl_2$ for 30 s at 4 °C).[19] Therefore, a wide range of polyamines enable the ribozyme to sample native-like conformations that are readily converted to the native structure in Mg^{2+}.

Highly charged polyamines are most effective

Multivalent metal cations stabilize the folded ribozyme more efficiently than monovalent cations, with a nearly 200-fold decrease in the midpoint of equilibrium folding transitions with each increment in the counterion charge.[19] The folding equilibrium of the *Tetrahymena* ribozyme at 30 °C was measured in varying concentrations of pentalysine^{5+}, spermine^{4+}, spermidine^{3+}, putrescine^{2+} (1,4-butanediamine) and ammonium^{+}. The midpoints of transitions from unfolded to folded ribozyme were lower when folding was induced by highly charged cations like pentalysine (4.5 μM) and spermine (6.2 μM), compared to putrescine (6 mM) and ammonium (530 mM) (Figure 3B, Table 1). The cooperativity of the transition with respect to cation concentration increased with the charge on the polyamine (Table 1).

Higher cooperativity corresponds to a larger free energy gap between the ensemble of "unfolded" structures present in Hepes buffer (U) and the native-like conformations (I_N), as shown in Table 1. Stabilization of the folded RNA can be explained by more complete neutralization of the phosphate charge in the presence of multivalent polyamines.[20] It is possible that various polyamines interact differently with the unfolded RNA, and this accounts for the observed differences in the free energy of folding. This explanation seems less likely, because even counterions that weakly drive folding, such as putrescine, associate more strongly with the folded RNA than the unfolded state under all conditions tested. We never observed unfolding of the RNA, even in 250 mM putrescine.

Polyamine size

As described in Introduction, the effective charge of a counterion is also related to its excluded volume. To understand how the size of counterions affect RNA tertiary structure, we compared folding reactions of the *Tetrahymena* ribozyme in a series of diamines, in which the positively charged amino groups are separated by two to five methylenes (Figure 1). As shown in Figure 4, the midpoint of the folding transition increased and the cooperativity decreased as the size of the diamine increased (Table 1). This resulted in a smaller Δ*G* for folding in large diamines, as expected. The stability of the RNA decreases nearly linearly with the average charge density of the cation, as the number of carbon atoms is increased from three to five (Figure 4C).

The transition induced by 1,2-ethanediamine (2C) was more cooperative than that of 1,3-propanediamine (3C). This resulted in a lower Δ*G* of folding in 1,2-ethanediamine than expected from its size alone (Figure 4C and Table 1). As

Table 1. Polyamine-dependent folding of the *Tetrahymena* L-21 ribozyme

Cation		C_m (M)[a]	n[a]	Δ*G* (kcal/mol)[b]	V_C (Å^3)[c]	$-\ln \phi$[c]	$\bar{\nu}$[d]
Pentalysine	+5	$4.5 \pm 1.7 \times 10^{-6}$	2.2 ± 0.3	−0.83 ± 0.06	1254.2	19.26	0.037
Spermine	+4	$6.2 \pm 0.2 \times 10^{-6}$	13 ± 2.8	−7.1 ± 1.6	469	20.15	0.046
Spermidine[e]	+3	$6.2 \pm 0.2 \times 10^{-5}$	7.5 ± 0.7	−4.0 ± 0.05	337	18.22	0.062
Ammonium	+1	$5.3 \pm 0.3 \times 10^{-1}$	5.1 ± 0.4	−3.0 ± 0.24	44.6	16.83	0.186
Ethanediamine	+2	$3.6 \pm 0.3 \times 10^{-3}$	4.5 ± 0.1	−2.6 ± 0.23	141.2	15.06	0.093
Propanediamine	+2	$3.4 \pm 0.2 \times 10^{-3}$	2.5 ± 0.1	−1.1 ± 0.1	174.5	14.91	0.093
Butanediamine	+2	$6.2 \pm 1.1 \times 10^{-3}$	2.2 ± 0.1	−0.89 ± 0.03	207.8	13.95	0.093
Pentanediamine	+2	$1.4 \pm 0.2 \times 10^{-2}$	2.0 ± 0.3	−0.74 ± 0.3	241.1	13.04	0.093

[a] Reactions at 30 °C in 25 mM Na–Hepes (pH 7.5), 1 mM EDTA. The midpoint (C_m) and Hill coefficient n were from fits to equation (2). Values are the average of two independent experiments.

[b] Δ*G* of polyamine-dependent folding transition was calculated from equation (3).

[c] The volume of the polyamine, V_C, is the sum of the van der Waal's volumes of the atoms. φ is the volume fraction of counterions in bulk solution at the midpoint of the transition, and is given by $\phi = N_A C V_C$, where N_A is the Avogadro's number and C is the concentration of cations at the midpoint.

[d] The average residual phosphate charge after counterion condensation, $\bar{\nu}$, was calculated from $\nu = b/l_B Z$, where b is the distance between phosphate groups (1.3 Å in *A*-form RNA), l_B is the Bjerrum length, and Z is the counterion charge.

[e] Folding parameters for spermidine were reported to be $C_m = 54$ μM and $n_H = 2.4 \pm 0.2$ by Heilman-Miller *et al.*[19]. We believe that these differences are due to transcription of the ribozyme in the presence of 2 mM spermidine at 37 °C in the present study. In the article by Heilman-Miller *et al.*[19], transcription reactions were at 30 °C and contained no spermidine.

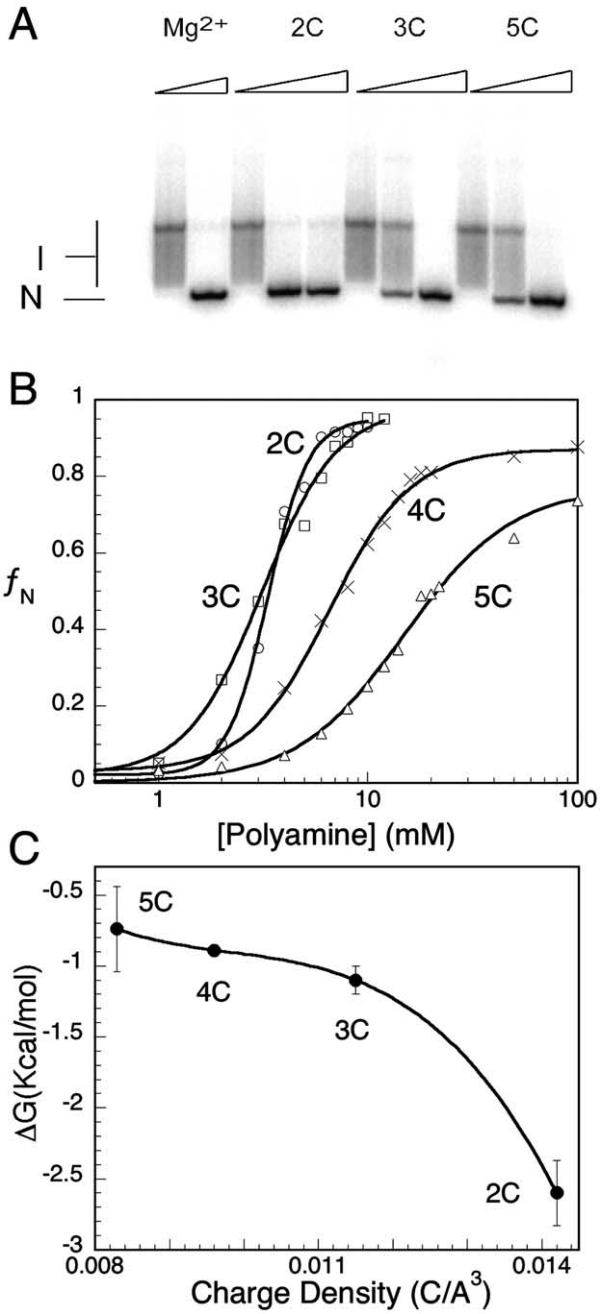

Figure 4. Equilibrium folding of the *Tetrahymena* ribozyme by different size diamines. A, Native 8% polyacrylamide gel, as in Figure 3A. HE, buffer only; Mg^{2+}, 1.2 mM $MgCl_2$. Polyamine concentrations: 2C, 0 mM, 3 mM, 8 mM 1,2 ethanediamine·$(HCl)_2$; 3C, 0 mM, 3 mM, 12 mM 1,3 propanediamine·$(HCl)_2$; 5C, 0 mM, 22 mM, 100 mM 1,5 pentanediamine·$(HCl)_2$. B, Fraction of native RNA (f_N) *versus* diamine concentration, as in Figure 3B. Parameters from the fits to equation (2) are shown in Table 1. Symbols: (○) 1,2-ethanediamine; (□) 1,3-propanediamine; (×) 1,4-butanediamine (putrescine); (△) 1,5-pentanediamine. (c) ΔG of folding (Table 1) *versus* the charge density of polyamines. The charge density of each polyamine was obtained by dividing the charge by the van der Waal's volume. The data were fit to a third order polynomial.

discussed below, the greater cooperativity of folding induced by 1,2-ethanediamine may be due to a favorable interaction geometry between the amine and RNA phosphate groups.

Brownian dynamics simulations of counterion-induced collapse

The experimental results above are consistent with the expectation that for a given counterion charge (Z), condensation efficiency decreases as the size of the counterion increases. To obtain qualitative insights into the dynamics of counterion-induced collapse, we carried out Brownian dynamics (BD) simulations of strongly charged polyelectrolyte chains. The RNA chain was modeled as a flexible chain of spherical monomers, each carrying a -1 charge (see Materials and Methods). Metal cations were represented as a single sphere with charge $+Z$ and polyamines represented as short flexible chains with a total charge $+Z$. Although they lack molecular detail, these simulations may be used to analyze the initial events in RNA folding corresponding to counterion-mediated collapse.

In all simulated trajectories (Table 2), the addition of counterions produced monomeric and compact globules of polyelectrolyte. The decay of the radius of gyration, R_g, as a function of time for a spherical trivalent counterion and a linear counterion with $Z = 3$ (Figure 5(a)) shows that collapse occurs more rapidly for the spherical counterion. This agrees with our current results and previous studies,[19] showing that $[CO(NH_3)_6]^{3+}$ is a more efficient condensing agent than spermidine^{3+}.

To understand the differences in the diamine series, we simulated the collapse of polyelectrolyte chains in the presence of counterions $P-A_X-P$, where P is positively charged and A is a neutral sphere that models the methylene group. Ethanediamine roughly corresponds to $X = 2$ while pentanediamine is modeled with $X = 5$. As shown in Figure 5(a), $P-A_5-P$ is less efficient in inducing chain collapse than $P-A_2-P$. These simulations support our interpretation of RNA collapse by the various diamine counterions (Table 1).

Although the diamines all have the same charge ($Z = 2$), the spacing between the positive charges

Table 2. Summary of simulations

N_v	Z	M_v	t_N (t_0)	Runs
40	3	1	500	10
40	3	3	500	10
60	2	4	1000	5
60	2	7	1000	5

N_v is the number of counterions; Z, valence of counterions; M_v, mass of counterions; $t_N(t_0)$, total run time; Runs, the number of independent trajectories.

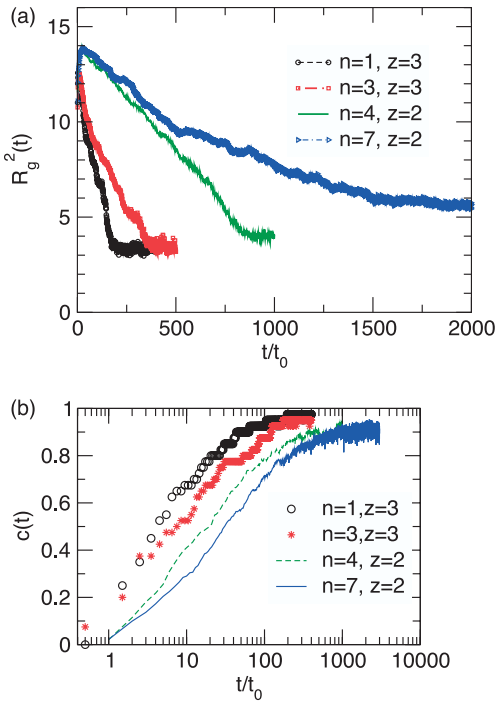

Figure 5. Brownian dynamics simulations of polyelectrolyte collapse. RNA and counterions were modeled as flexible chains of spherical residues, as described in Materials and Methods. Counterions were $[Co(NH_3)_6]^{3+}$, $Z = 3$, $n = 1$ (black); spermidine, $Z = 3$, $n = 3$ (red); 1,2-ethanediamine, $Z = 2$, $n = 4$; 1,5-pentanediamine, $Z = 2$, $n = 7$ (blue). (a) Decrease in R_g^2 as a function of time t/t_0, where $t_0 = a^2/D$, the ion diffusion constant. For $a = 6.3$ Å and $D = 10^{-6}$ cm^2 s^{-1}, $t_0 \approx 4$ ns. R_g was calculated using $R_g^2 = 1/2N^2\sum r_{ij}^2$, where N is the number of monomers and r_{ij} is the distance between i and j monomers. (b) Fraction of condensed counterions around the polyelectrolyte *versus* time.

affected the collapse time-scale and the nature of the compact conformations. Examination of the structures sampled during each simulation showed that for the counterion P–A_2–P highly compact structures appear early, whereas such structures form on a longer time-scale when the counterion is P–A_5–P. In addition, the final extent of compaction depends on the number of methylene groups separating the positive charges. As discussed below, collapse is most efficient for a given Z if the spacing between positive charges in the polyamine is commensurate with the distance between the phosphate groups in the native RNA.

An important question that is difficult to answer experimentally is the extent of neutralization of the phosphate charge upon counterion condensation. Manning–Oosawa theory predicts that for RNA, more than 90% of the phosphate charge is neutralized by non-specific counterion condensation, if $Z \geq 2$ (Table 1). Using BD simulations, we calculated the time dependence of the counterion condensation for cations modeling $[Co(NH_3)_6]^{3+}$, spermidine, ethanediamine and pentanediamine. In all cases, in excess of 80% of the backbone charges are neutralized at long times, when chain collapse is nearly complete (Figure 5(b)). The efficiency with which a particular counterion induces chain collapse agrees with the extent of charge neutralization predicted by counterion-condensation theory. Comparison of the results in Figure 5(a) and (b) also shows that counterion condensation is faster than chain compaction.

Discussion

Stabilization of the folded RNA by multivalent polyamines

The concentration of multivalent counterions needed to induce collapse of highly charged polyelectrolytes is much less than for monovalent ions. For polyamines tested in this study, each additional unit of charge lowers the midpoint of the folding transition approximately 100-fold (Table 1). The midpoints are roughly consistent with the net entropy gain expected for the release of Na^+into the bulk solution when polyamines associate with the RNA.[43] Competitive binding, however, does not explain the greater cooperativity of RNA folding in multivalent ions. This increase in cooperativity can be explained by charge fluctuations, as the magnitude of the attractive potential increases with the square of the counterion charge. For a trivalent counterion in 1 mM monovalent salt, and $b = 1.7$ Å (see Materials and Methods), it was calculated that the addition of 10–100 μM counterion was sufficient to induce chain collapse, in agreement with our experimental observations.[34]

Size of polyamine: importance of excluded volume

Comparison of the ΔG and C_m values for diamine series vividly illustrates the importance of the excluded volume on the thermodynamics of RNA folding. Experimental and theoretical work on the association of polyamines with double-stranded DNA suggests how the size of the counterion can influence electrostatic interactions with the nucleic acid.[15,29,35,44] First, counterions with a large radius cannot approach the nucleic acid as closely as smaller ions, resulting in weaker Coulombic interactions between the phosphate groups and the counterions, and weaker competitive binding with monovalent ions. Second, the number of counterions in the condensed layer around the nucleic acid depends on the excluded volume of the ions.

As fewer counterions with a large excluded volume, these ions shield the negative charge of the phosphate groups less effectively than smaller diamines or NH_4^+, and are less able to stabilize near-native RNA structures. The difficulty of

fully neutralizing the phosphate charge with large ions may explain incomplete folding (65%) in pentalysine and 1,5-pentanediamine, two counterions with a large excluded volume and low charge density.

Is spatial correlation between territorially bound counterions relevant for RNA folding?

The non-monotonic dependence of C_m and cooperativity on diamine size (Table 1) suggests that spatial correlations between the non-specifically bound cations also play a role in the stability of the folded RNA. If the counterions are separated by a distance σ that is larger than the Debye length ($\sigma/\lambda_D > 1$, where $\lambda_D = (8\pi l_B I)^{-1/2}$ and is the ionic strength), then the mobile but bound counterions may be considered independent. In the opposite limit ($\sigma/\lambda_D < 1$), the bound counterions interact with each other and should be treated as a correlated fluid. In the latter situation, the bulky counterions do not approach the RNA closely enough to efficiently neutralize the backbone charge. Moreover, because of spatial correlation between the bound ions, there may be anticooperativity in the condensation process itself. These factors explain the dramatically lower cooperativity and nearly fourfold increase in C_m, in going from pentanediamine to ethanediamine. In addition, bulky counterions should lead to less compact structures. This prediction can be validated using small angle X-ray scattering experiments.

Geometry of counterion interactions

Besides excluded volume effects and spatial correlations between bound counterions, the spacing between the charged groups in the polyamines may also affect RNA folding (Figure 6). As polyamines principally interact with the phosphate groups in RNA, binding should be optimal when each amino group can be placed near a phosphate. The average distance between the two amino groups in 1,2-ethanediamine, assuming a *trans* conformation, is 5.3 Å. This is similar to the typical distance (5.5–6 Å) between phosphate groups in RNA structures found in the Protein Databank. This geometric advantage may explain why ethanediamine stabilizes the *Tetrahymena* ribozyme more than expected based on its size and valence. A similar explanation was offered for the relative stabilization of polyA·polyU and polyI·polyC by simple diamines.[36]

On the other hand, 1,5-pentanediamine has more degrees of freedom than 1,2-ethanediamine in the bulk solution, and experiences a greater loss of entropy when it interacts with two adjacent phosphate groups on the RNA. Moreover, the volume excluded by large counterions may eventually inhibit the close packing of RNA double helices necessary to achieve the native structure of the ribozyme.[45]

Conclusions

The results presented here show that the cooperativity of the folding transition of the *Tetrahymena* ribozyme to native-like structures reflects a hierarchy of interactions that depend on the valence and size of the counterions. The efficiency with which a counterion induces RNA collapse depends on the charge density of the counterion, which reflects both the volume excluded by the counterions and spatial correlations between counterions. While the

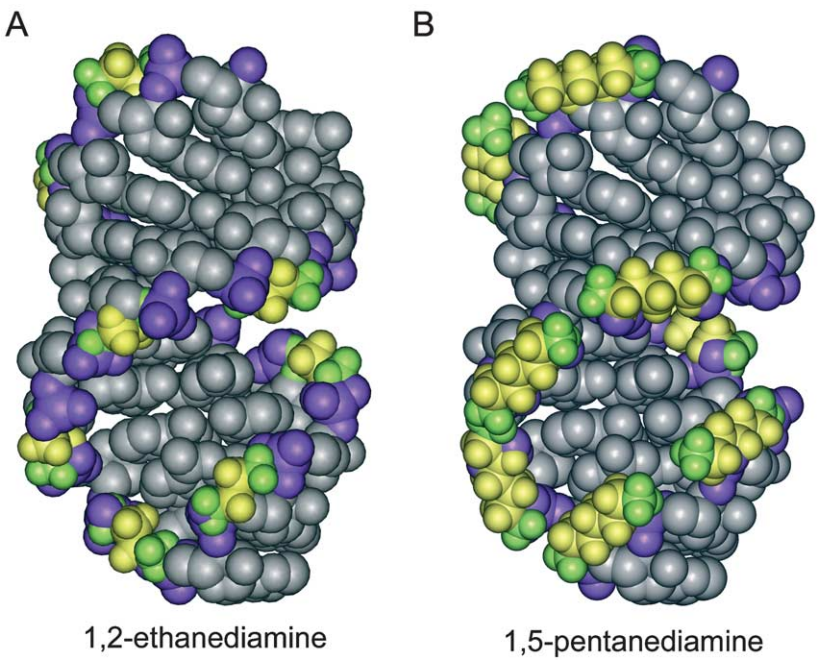

Figure 6. Interaction of polyamines with RNA. Interaction of polyamines with nt 141–161 of the *Tetrahymena* ribozyme (P5b) were modeled with Insight II (Molecular Simulations). A, 1,2-Ethanediamine; B, 1,5-pentanediamine. Space-filling model with RNA in gray; phosphate groups, violet; amino groups, green; methylenes, yellow. The coordinates for the RNA[47] (1HR2) were obtained from the Protein Data Bank (http://www.rcsb.org/pdb/). 1,5-Pentanediamine molecules are closer and repulse each other more than 1,2-ethanediamine when associated with RNA phosphate groups. Consequently, 1,5-pentanediamine creates higher energy RNA structures.

attractive potential arising from correlated charge fluctuations increases with the square of counterion charge, entropic forces that oppose packing of large counterions around the RNA reduce the cooperativity of the folding transition. Because the ensemble of compact RNA structures can vary depending on the chemical structure of the counterions, changes in intracellular salt concentrations or levels of polyamines are likely to modulate RNA folding pathways *in vivo*.

Materials and Methods

Reagents

Spermine tetrahydrochloride was purchased from Fluka. All other chemicals were purchased from Sigma-Aldrich.

RNA folding reactions

Uniformly α-^{32}P-labeled L-21 RNA was prepared as described.[19] The RNA was incubated in HE buffer (50 mM Hepes adjusted to pH 7.5 with sodium hydroxide, 1 mM EDTA (pH 8.5)), 10% (v/v) glycerol, 0.1% (w/v) xylene cyanol, plus the desired concentration of polyamine hydrochloride. The reactions were incubated for two to four hours at 30 °C. A 2 μl aliquot of each reaction was loaded on a cold native 8% polyacrylamide gel (<10 °C) as described.[9,14,25] Native gels were quantified using a Molecular Dynamics Phosphorimager as described.[14] The fraction of native RNA at each concentration of polyamines was obtained from the ratio of the counts in the native band over the total counts in the lane. The fraction of native RNA *versus* the cation concentration was fit to the Hill equation:

$$f_N = f_N(0) + [f_N(\max) - f_N(0)]\left[\frac{(C/C_m)^n}{1+(C/C_m)^n}\right] \quad (2)$$

where $f_N(0)$ is the fraction of folded RNA at zero polyamine concentration, $f_N(\max)$ is the maximum fraction of folded RNA, C_m is the midpoint in the folding transition and n is the Hill coefficient. The free energy of the folding transition was calculated from:

$$\Omega_C = \frac{1}{8}\left(\frac{\Delta G_{UN}}{RT}\right)^2 \frac{1}{\ln(3+2\sqrt{2})} = \frac{C_{max}^2 (df_N/dC)_{max}}{\Delta C} \quad (3)$$

where R is the gas constant, T is temperature, and ΔG_{UN} is the free energy of the polyamine dependent folding transition.[20] Ω_C is a dimensionless quantity that is related to the Hill coefficient and the midpoint of folding transition, C_{max} is the concentration of polyamine at which the derivative of fraction native with respect to the concentration of polyamine reaches its maximum, $(df_N/dC)_{max}$ is the maximum value of the derivative, ΔC is the width of the curve at $1/2(df_N/dC)_{max}$. (df_N/dC) was determined analytically from the Hill coefficient and the midpoint of the folding transition.

Brownian dynamics simulations

Polyelectrolyte (PE) chains were represented as a flexible chain of 120 monomers, with each one carrying a charge of −1e. Each monomer had a van der Waal's radius of $a/2$. Successive monomers were connected by a spring with spring constant $80RT/a^2$ ($RT = 0.6$ kcal/mol and $a = 6.3$ Å). Counterions were added to the system to achieve charge neutrality (total positive charge = +1e). $[Co(NH_3)_6]^{3+}$ was represented by a single sphere with $Z = 3$, spermidine as three spheres with $Z = 1$ (P–P–P) and diamines by P–A_X–P, where P is positively charged and A is a neutral sphere.

Coulombic interactions between charge pairs were treated by accounting for images using a real space Ewald sum. Attractive interactions between the monomers were represented by standard Lennard–Jones potentials. The potentials used to mimic these interactions and the details of the simulations are nearly the same as used in our previous study.[46] For each system, five to ten trajectories were produced so that statistical errors were minimized. The simulation times ($t_N(t_0) = 500$ or 1000) were long enough to observe collapse of the chain into a globular structure.

Interphosphate distances

The distance between phosphate groups in RNA structures deposited in the Protein Data Bank† was computed from the distance between the center of mass of phosphate groups within a cutoff distance of 10 Å.

Acknowledgements

This work was supported by a grant from the NIH (GM46686 to S.W.) and the NSF (CHE02-09340 to D.T.).

References

1. Misra, V. K. & Draper, D. E. (1998). On the role of magnesium ions in RNA stability. *Biopolymers*, **48**, 113–135.
2. Tabor, C. W. & Tabor, H. (1984). Polyamines. *Annu. Rev. Biochem.* **53**, 749–790.
3. Draper, D. E. (1999). Themes in RNA–protein recognition. *J. Mol. Biol.* **293**, 255–270.
4. Childs, A. C., Mehta, D. J. & Gerner, E. W. (2003). Polyamine-dependent gene expression. *Cell Mol. Life Sci.* **60**, 1394–1406.
5. Igarashi, K. & Kashiwagi, K. (2000). Polyamines: mysterious modulators of cellular functions. *Biochem. Biophys. Res. Commun.* **271**, 559–564.
6. Matsufuji, S., Matsufuji, T., Miyazaki, Y., Murakami, Y., Atkins, J. F., Gesteland, R. F. & Hayashi, S. (1995). Autoregulatory frameshifting in decoding mammalian ornithine decarboxylase antizyme. *Cell*, **80**, 51–60.
7. Ivanov, I. P., Matsufuji, S., Murakami, Y., Gesteland, R. F. & Atkins, J. F. (2000). Conservation of polyamine regulation by translational frameshifting from yeast to mammals. *EMBO J.* **19**, 1907–1917.
8. Thomas, T. & Thomas, T. J. (2003). Polyamine metabolism and cancer. *J. Cell. Mol. Med.* **7**, 113–126.
9. Bloomfield, V. A., Wilson, R. W. & Rau, D. C. (1980). Polyelectrolyte effects in DNA condensation by polyamines. *Biophys. Chem.* **11**, 339–343.

† http://www.rcsb.org/pdb/

10. Hampel, K. J., Crosson, P. & Lee, J. S. (1991). Polyamines favor DNA triplex formation at neutral pH. *Biochemistry*, **30**, 4455–4459.
11. Thomas, T. & Thomas, T. J. (1993). Selectivity of polyamines in triplex DNA stabilization. *Biochemistry*, **32**, 14068–14074.
12. Antony, T., Thomas, T., Shirahata, A. & Thomas, T. J. (1999). Selectivity of polyamines on the stability of RNA–DNA hybrids containing phosphodiester and phosphorothioate oligodeoxyribonucleotides. *Biochemistry*, **38**, 10775–10784.
13. Jain, S., Zon, G. & Sundaralingam, M. (1989). Base only binding of spermine in the deep groove of the A-DNA octamer d(GTGTACAC). *Biochemistry*, **28**, 2360–2364.
14. Quigley, G. J., Teeter, M. M. & Rich, A. (1978). Structural analysis of spermine and magnesium ion binding to yeast phenylalanine transfer RNA. *Proc. Natl Acad. Sci. USA*, **75**, 64–68.
15. Braunlin, W. H., Strick, T. J. & Record, M. T., Jr (1982). Equilibrium dialysis studies of polyamine binding to DNA. *Biopolymers*, **21**, 1301–1314.
16. Wemmer, D. E., Srivenugopal, K. S., Reid, B. R. & Morris, D. R. (1985). Nuclear magnetic resonance studies of polyamine binding to a defined DNA sequence. *J. Mol. Biol.* **185**, 457–459.
17. Deng, H., Bloomfield, V. A., Benevides, J. M. & Thomas, G. J., Jr (2000). Structural basis of polyamine–DNA recognition: spermidine and spermine interactions with genomic B-DNAs of different GC content probed by Raman spectroscopy. *Nucl. Acids Res.* **28**, 3379–3385.
18. Bloomfield, V. A. (1991). Condensation of DNA by multivalent cations: considerations on mechanism. *Biopolymers*, **31**, 1471–1481.
19. Heilman-Miller, S. L., Thirumalai, D. & Woodson, S. A. (2001). Role of counterion condensation in folding of the *Tetrahymena* ribozyme. I. Equilibrium stabilization by cations. *J. Mol. Biol.* **306**, 1157–1166.
20. Pan, J., Thirumalai, D. & Woodson, S. A. (1999). Magnesium-dependent folding of self-splicing RNA: exploring the link between cooperativity, thermodynamics, and kinetics. *Proc. Natl Acad. Sci. USA*, **96**, 6149–6154.
21. Thirumalai, D., Lee, N., Woodson, S. A. & Klimov, D. (2001). Early events in RNA folding. *Annu. Rev. Phys. Chem.* **52**, 751–762.
22. Buchmueller, K. L., Webb, A. E., Richardson, D. A. & Weeks, K. M. (2000). A collapsed, non-native RNA folding state. *Nature Struct. Biol.* **7**, 362–366.
23. Fang, X., Littrell, K., Yang, X. J., Henderson, S. J., Siefert, S. & Thiyagarajan, P. (2000). Mg^{2+}-dependent compaction and folding of yeast tRNAPhe and the catalytic domain of the *B. subtilis* RNase P RNA determined by small-angle X-ray scattering. *Biochemistry*, **39**, 11107–11113.
24. Russell, R., Millett, I. S., Doniach, S. & Herschlag, D. (2000). Small angle X-ray scattering reveals a compact intermediate in RNA folding. *Nature Struct. Biol.* **7**, 367–370.
25. Russell, R., Millett, I. S., Tate, M. W., Kwok, L. W., Nakatani, B., Gruner, S. M. *et al.* (2002). Rapid compaction during RNA folding. *Proc. Natl Acad. Sci. USA*, **99**, 4266–4271.
26. Perez-Salas, U. A., Rangan, P., Krueger, S., Briber, R. M., Thirumalai, D. & Woodson, S. A. (2004). Compaction of a bacterial group I ribozyme coincides with the assembly of core helices. *Biochemistry*, **43**, 1746–1753.
27. Manning, G. S. (1978). The molecular theory of polyelectrolyte solutions with applications to the electrostatic properties of polynucleotides. *Quart. Rev. Biophys.* **11**, 179–246.
28. Bloomfield, V. A. (1997). DNA condensation by multivalent cations. *Biopolymers*, **44**, 269–282.
29. Rouzina, I. & Bloomfield, V. A. (1996). Influence of ligand spatial organization on competitive electrostatic binding to DNA. *J. Phys. Chem.* **100**, 4305–4313.
30. Nguyen, T. T., Rouzina, I. & Shklovskii, B. I. (2000). Reentrant condensation of DNA induced by multivalent counterions. *J. Chem. Phys.* **112**, 2562–2568.
31. Anderson, C. F. & Record, M. T. (1995). Salt nucleic-acid interactions. *Annu. Rev. Phys. Chem.* **46**, 657–700.
32. Misra, V. K. & Draper, D. E. (2002). The linkage between magnesium binding and RNA folding. *J. Mol. Biol.* **317**, 507–521.
33. Misra, V. K. & Draper, D. E. (1999). The interpretation of $Mg(2+)$ binding isotherms for nucleic acids using Poisson–Boltzmann theory. *J. Mol. Biol.* **294**, 1135–1147.
34. Ha, B. Y. & Thirumalai, D. (2003). Bending rigidity of stiff polyelectrolyte chains: a single chain and bundle of multichains. *Macromolecules*, **36**, 9658–9666.
35. Stigter, D. & Dill, K. A. (1996). Binding of ionic ligands to polyelectrolytes. *Biophys. J.* **71**, 2064–2074.
36. Glasser, R. & Gabbay, E. J. (1968). Topography of nucleic acid helices in solutions. 3. Interactions of spermine and spermidine derivatives with polyadenylic–polyuridylic and polyinosinic–polycytidylic acid helices. *Biopolymers*, **6**, 243–254.
37. Baumann, C. G., Smith, S. B., Bloomfield, V. A. & Bustamante, C. (1997). Ionic effects on the elasticity of single DNA molecules. *Proc. Natl Acad. Sci. USA*, **94**, 6185–6190.
38. Plum, G. E., Arscott, P. G. & Bloomfield, V. A. (1990). Condensation of DNA by trivalent cations. 2. Effects of cation structure. *Biopolymers*, **30**, 631–643.
39. Raspaud, E., Olvera de la Cruz, M., Sikorav, J. L. & Livolant, F. (1998). Precipitation of DNA by polyamines: a polyelectrolyte behavior. *Biophys. J.* **74**, 381–393.
40. Vijayanathan, V., Thomas, T., Shirahata, A. & Thomas, T. J. (2001). DNA condensation by polyamines: a laser light scattering study of structural effects. *Biochemistry*, **40**, 13644–13651.
41. Pan, J., Deras, M. L. & Woodson, S. A. (2000). Fast folding of a ribozyme by stabilizing core interactions: evidence for multiple folding pathways in RNA. *J. Mol. Biol.* **296**, 133–144.
42. Emerick, V. L. & Woodson, S. A. (1994). Fingerprinting the folding of a group I precursor RNA. *Proc. Natl Acad. Sci. USA*, **91**, 9675–9679.
43. Record, M. T., Jr, Anderson, C. F. & Lohman, T. M. (1978). Thermodynamic analysis of ion effects on the binding and conformational equilibria of proteins and nucleic acids: the roles of ion association or release, screening, and ion effects on water activity. *Quart. Rev. Biophys.* **11**, 103–178.
44. Padmanabhan, S., Brushaber, V. M., Anderson, C. F. & Record, M. T., Jr (1991). Relative affinities of divalent polyamines and of their *N*-methylated analogues for helical DNA determined by 23Na NMR. *Biochemistry*, **30**, 7550–7559.
45. Doudna, J. A. & Doherty, E. A. (1997). Emerging themes in RNA folding. *Fold. Des.* **2**, R65–R70.
46. Lee, N. & Thirumalai, D. (2001). Dynamics of collapse of flexible polyelectrolytes in poor solvents. *Macromolecules*, **34**, 3446–3457.

47. Juneau, K., Podell, E., Harrington, D. J. & Cech, T. R. (2001). Structural basis of the enhanced stability of a mutant ribozyme domain and a detailed view of RNA–solvent interactions. *Structure*, **9**, 221–231.

Edited by J. Doudna

(Received 15 March 2004; received in revised form 28 May 2004; accepted 2 June 2004)